MDPI

Exploring the Dual Inhibitory Activity of Novel Anthranilic Acid Derivatives towards α-Glucosidase and Glycogen Phosphorylase Antidiabetic Targets: Design, In Vitro Enzyme Assay, and Docking Studies

Saleh Ihmaid

Pharmacognosy and Pharmaceutical Chemistry Department, Pharmacy College, Taibah University, Al-Madinah Al-Munawarah 41477, Saudi Arabia; sihmaid@taibahu.edu.sa

check for updates

Abstract: A few new anthranilate diamide derivatives, **3a–e**, **5a–c** and **7a–d**, were designed, synthesized, and evaluated for their inhibitory activity against two interesting antidiabetic targets, α-glucosidase and glycogen phosphorylase enzymes. Different instrumental analytical tools were applied in identification and conformation of their structures like; ^{13}C NMR, ^{1}H NMR and elemental analysis. The screening of the novel compounds showed potent inhibitory activity with nanomolar concentration values. The most active compounds (**5c**) and (**7b**) showed the highest inhibitory activity against α-glucosidase and glycogen phosphorylase enzymes IC_{50} = 0.01247 ± 0.01 μM and IC_{50} = 0.01372 ± 0.03 μM, respectively. In addition, in vivo testing of the highly potent α-glucosidase inhibitor (**7b**) on rats with DTZ-induced diabetes was done and showed significant reduction of blood glucose levels compared to the reference drug. Furthermore, a molecular docking study was performed to help understand the binding interactions of the most active analogs with these two enzymes. The data obtained from the molecular modeling were correlated with those obtained from the biological screening. These data showed considerable antidiabetic activity for these newly synthesized compounds.

Keywords: antidiabetic; anthranilate diamide; α-Glucosidase; glycogen phosphorylase; structure–activity relationships; molecular docking

1. Introduction

Diabetes mellitus disease is a chronic condition in which the human body is unable to produce adequate insulin hormone type 1 or is a hyperglycemia that is uncontrolled with endogenous available insulin type 2 and clinically characterized by aberrant elevated levels of glucose in the blood [1–3]. The degree of this problem is exemplified in the fact that type 2 diabetes is now becoming prevalent in children and adolescents [4,5]. It has become a major danger to global health, and represents an enormous social and economic problem. According to the World Health Organization (WHO), diabetes is the third-highest risk factor for premature death, after hypertension and cigarette smoking (WHO) [6]. In most countries, an increased prevalence of type 2 diabetes is associated with increasing urbanization, ageing populations, increased sugar intake, obesity, and low fruit and vegetable consumption [7–11]. Adequate management of this debilitating disease in many diabetic patients ultimately requires insulin treatment [12]. Although there are several treatment options for type 2 diabetes, the long-term efficacy of oral antidiabetic agents has been limited. It has recently been reported that 21% of patients will fail on metformin treatment within five years [13,14]. Currently, 14 classes of drugs are available to treat type 2 diabetes mellitus, but only 36% of patients with type 2 diabetes achieve glycemic control with the currently available therapies.
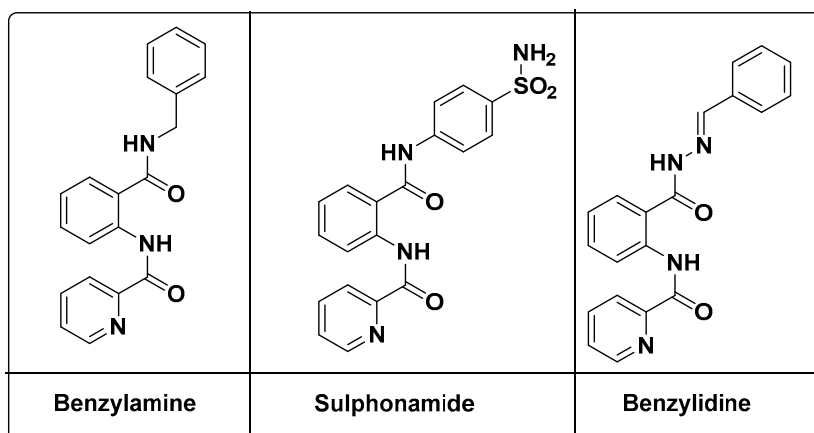
Therefore, new treatment options are desperately needed [15]. In the carbohydrate metabolism, excessive hepatic glucose production is a major component of hyperglycemia and consists of both glycogenolysis and gluconeogenesis. In the postprandial state glycogenolysis was more than doubled in diabetic subjects compared to non-diabetics. In addition, diabetics have a 55% reduction in liver glycogen content compared to normal subjects [16,17]. The enzyme glycogen phosphorylase a (GPa) is responsible for the release of glucose-1-phosphate from glycogen and is the rate-determining step in glycogenolysis. GPa has therefore become a target for glucose lowering in type 2 diabetes. Although several groups have reported small molecule inhibitors of GPa, definitive clinical results have not been communicated [18–20]. Glucosidase is an enzyme secreted from the intestinal chorionic epithelium and responsible for carbohydrate hydrolysis [21]. Therefore, glucosidase is a therapeutic target for many types of antidiabetic drugs having inhibitory activity against it, such as acarbose, miglitol, and voglibose, which are used in clinic for treatment of type 2 diabetes [22]. Recently, the molecules that were based on anthranilic acid scaffold have gained much attention in drug discovery and development [23–25]. Anthranilic acid and its derivatives are constituents of many bioactive molecules. Indeed, the anthranilic acid nucleus serves as a privileged substructure in the synthesis of amino acid tryptophan and its analogs, and also as a constituent of various alkaloids [26,27]. Both experimental and preclinical studies demonstrated the medicinal properties of anthranilic acid derivatives, including matrix metalloproteinase inhibition, anticancer, anti-inflammatory, and analgesic activities [28–32]. In a previous study, the potential antiglycating effect of an anthranilic acid derivative was identified in multiple stages of a non-enzymatic glycation process [33]. Lately, diamide derivatives have received significant attention for their glycogen phosphorylase inhibitor activities, especially those bearing a basic diamide scaffold and pharmacophores [34]. Various diamide derivatives have been reported for their wide range of pharmacological activities including antidiabetic activity [35–38]. The promising bioactive diversity of this class of diamide compounds urges us to synthesize and biologically evaluate a series of novel structural variants of anthranilic diamide derivatives as antidiabetic agents. In the present study, as compared to the reported anthranilic acid potent derivative, substitution of the substituted aniline derivatives with the pyridyl moiety might lead to the stability of a compound with consistent lipophilicity. In addition, the terminal amino acid fragment will be replaced with different aromatic substructures capable of forming hydrogen bonding and aromatic interactions through various linkers (Figure 1).

Figure 1. *Cont.*

Figure 1. Structural similarities and pharmacophoric features of reported and designed anthranilate diamides as antidiabetic agents compared to the reported reference drug.

2. Results and Discussion

2.1. Chemistry

Methyl 2-(picolinamido)benzoate (**1**) was synthesized with good yield (90–95%) from the reaction of methyl 2-aminobenzoate with picolinoyl chloride, in the presence of triethylamine (Et$_3$N) as catalyst in refluxing dimethylformamide (DMF), the according to the previously reported procedure with no further modification [32] (Scheme 1). The structure of the product (**1**) was confirmed from the analysis of their IR, ^{1}H, ^{13}C neuclear magnetic resonance (NMR) spectra in addition to microanalysis (see experimental Section 3.2).
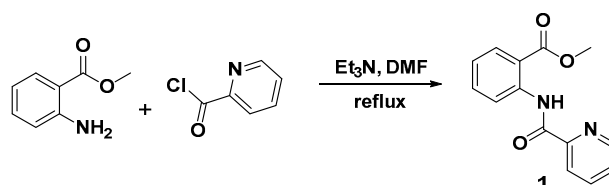
Scheme 1. Synthesis of methyl 2-(picolinamido)benzoate (**1**).

The reaction of methyl 2-(picolinamido)benzoate (**1**) with benzylamine derivatives and sulfa derivatives in the presence of potassium tert-butoxide in acetonitrile led to the synthesis of *N*-(2-((4-substiutedbenzyl)carbamoyl)phenyl)picolinamide **3a–e** with yields of 80–95% and *N*-(2-((4-sulfasubstitutedphenyl)carbamoyl)phenyl)picolinamide **5a–c** with yields of 80–85% (Scheme 2). The structures of the new products **3a–e, 5a–c** were confirmed from their infrared (IR), ^{1}H nuclear magnetic resonance (NMR), and ^{13}C nuclear magnetic resonance (NMR) and microanalysis (see experimental Section 3.3).

The *N*-(2-(hydrazinecarbonyl)phenyl)pyridine-2-carboxamide (**6**), as prepared from the reaction of methyl 2-(picolinamido)benzoate (**1**) with hydrazine hydrate in refluxing ethanol for 8 h, afforded the targeted *N*-(2-(hydrazinecarbonyl)phenyl)pyridine-2-carboxamide (**6**) in 95% yield according to the previously reported procedures [32] (Scheme 2). The structure of the new product (**6**) was confirmed by the analysis of their infrared (IR), ^{1}H nuclear magnetic resonance (NMR), and ^{13}C nuclear magnetic resonance (NMR) spectroscopy in addition to the microanalysis (see experimental Section 3.4). Schiff bases were synthesized by heating under reflux the acid hydrazide (**6**) with appropriate aromatic aldehydes in the presence of ethanol as solvent and hydrochloric acid (HCl) as catalyst (Scheme 2). The structures of new Schiff bases **7a–d** were confirmed by the analysis of their infrared (IR), ^{1}H nuclear

magnetic resonance (NMR), and ^{13}C nuclear magnetic resonance (NMR) spectroscopy in addition to the microanalysis (see experimental Section 3.5).
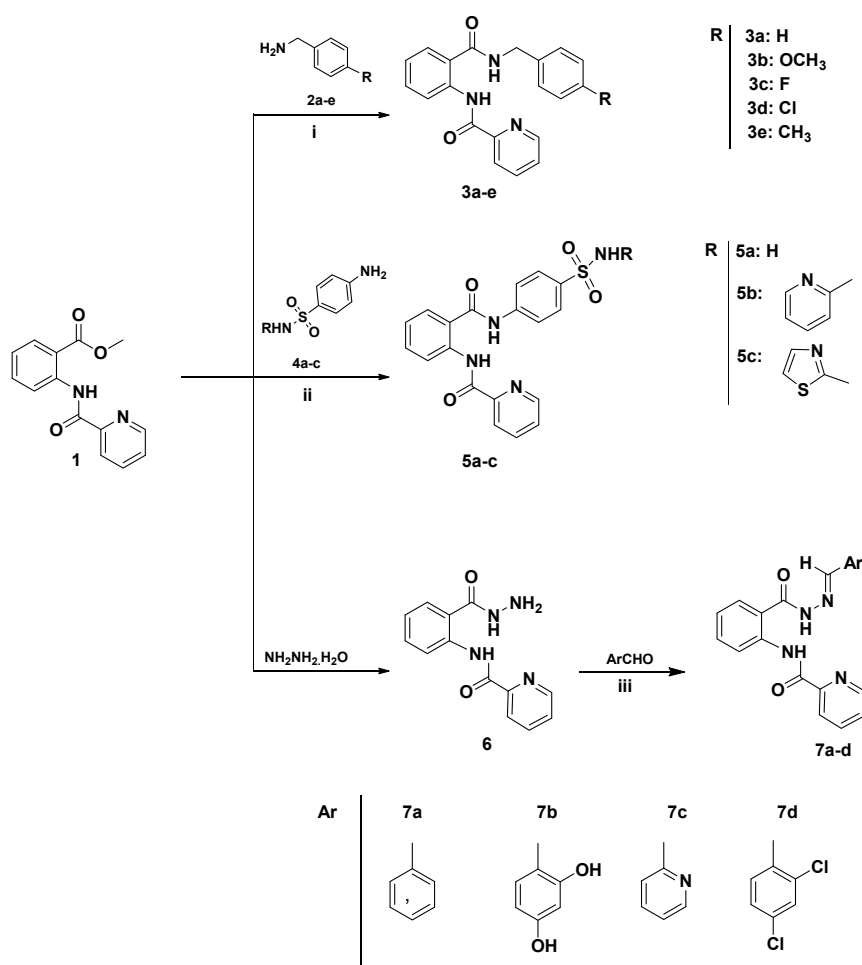
Scheme 2. The reactions of the methyl 2-(picolinamido)benzoate (**1**) with benzylamine derivatives, sulfa derivatives and aromatic aldehyde derivatives, respectively. Reaction conditions: (**i**) potassium tert-butoxide in acetonitrile and reflux; (**ii**) potassium tert-butoxide in acetonitrile and reflux; (**iii**) EtOH, HCl, and reflux.

2.2. Biological Screening

2.2.1. α-Glucosidase Inhibitory Assay

All compounds were evaluated with regard to α-glucosidase inhibition and the resulted data are reported in (Table 1). Generally, they showed inhibition at various nanomolar concentrations. Some significant inhibitory effects were detected for the title compounds (**1**) and (**7**), IC_{50} = 0.735 and IC_{50} = 0.416 μM, respectively. All tested compounds showed more inhibitory activity than the parent diamides by a range of IC_{50} = 0.0124 to IC_{50} = 0.231 μM. The order of inhibitory behavior of compounds was sorted as follows: benzylamine derivatives **3b** > **3e** > **3a** > **3d** > **3c**, sulfonamide derivatives **5c** > **5b** > **5a**, and last benzylidine series **7b** > **7a** > **7d** > **7c**. Among these compounds, the derivatives of (**5c**), (**7b**), (**5b**) and (**3b**) showed the most potent anti-α-glucosidase enzyme effect with inhibitory concentrations. It was clear that compound (**5c**) IC_{50} = 0.01247 μM was the most active unique sulfonamide analog, bearing a six-membered aromatic heterocyclic ring pyridine substructure. Of these active analogs, two selective α-glucosidase inhibitors (**7a**) non-substituted aromatic benzylidine derivative and (**3e**) 4-methyl benzyl derivative with activity

profile towards this enzyme and less potent against the glycogen phosphorylase one, $IC_{50} = 0.0445$ and $IC_{50} = 0.0708$ respectively. However, compounds (**7d**) $IC_{50} = 0.07842$ µM and (**5a**) $IC_{50} = 0.0477$ µM displayed slight equal potency against the two target enzymes (Figure 2A).

Table 1. Inhibitory data of the target compounds to both α-glucosidase and glycogen phosphorylase.

Compounds	IC50 (µM)		Scaffold
	α-Glucosidase	Glycogen Phosphorylase	
1	0.7355 ± 2.4	0.5415 ± 0.06	*N*-Furoylanthranilate (NFA)
3a	0.0896 ± 1.52	0.1502 ± 0.07	
3b	0.0223 ± 0.08	0.01808 ± 0.84	
3c	0.0585 ± 7.57	0.08639 ± 0.02	Benzyl NFA
3d	0.0947 ± 0.68	0.1774 ± 0.05	
3e	0.0708 ± 14.2	0.262 ± 0.01	
5a	0.0477 ± 0.59	$0.07047 \pm 0,01$	
5b	0.0212 ± 0.07	0.0166 ± 0.09	Sulfonamide NFA
5c	0.01247 ± 0.01	0.02291 ± 0.57	
6	0.4166 ± 11.4	0.5818 ± 0.58	NFA-Hydrazine
7a	0.0445 ± 12.1	0.2078 ± 2.57	
7b	0.0176 ± 0.09	0.01372 ± 0.03	
7d	$0.07842 \pm .05$	0.054 ± 5.14	Benzylidine NFA
7c	0.2313 ± 0.57	0.0367 ± 2.56	
1-Deoxynojirimycin	0.01011 ± 1.81	0.0556 ± 0.11	-
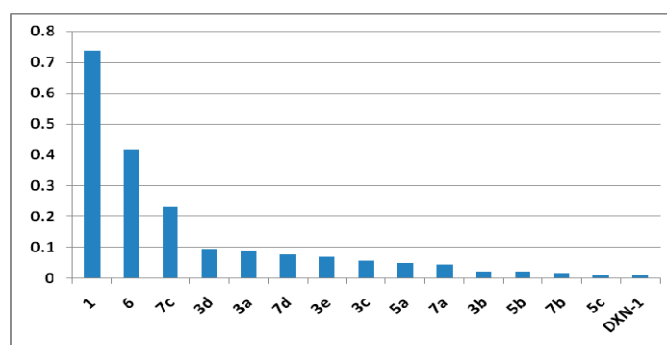
(**A**)
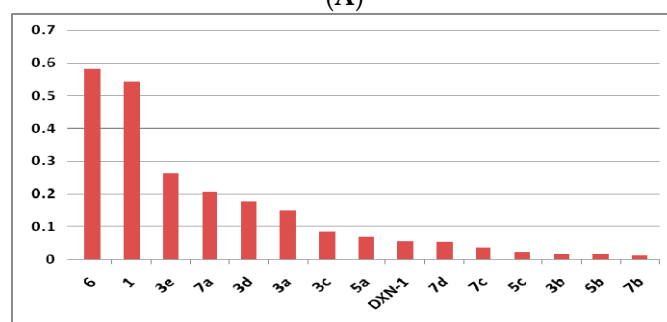
(**B**)

Figure 2. Bar chart of the inhibitory activity data of target compounds sorted from lowest activity to highest against two antidiabetic drug enzymes compared to the reference drug: (**A**) α-glucosidase; (**B**) glycogen phosphorylase.

2.2.2. Glycogen Phosphorylase Inhibitory Assay

The new compounds were assayed against rabbit muscle glycogen phosphorylase, as described in the experimental Section 3.7, and the results are reported in (Table 1). The order of activity of target compounds assayed against the glycogen phosphorylase enzyme was: benzylamine derivatives **3b** > **3c** > **3a** > **3d** > **3e**, sulfonamide derivatives **5b** > **5c** > **5a**, and last benzylidine series **7b** > **7c** > **7d** > **7a**. The inhibitory profile of these compounds ranged between IC_{50} = 0.01372 and IC_{50} = 0.5818 μM. The class benzylidine derivatives are slightly more potent than the sulfonamide ones and the benzylamine analogs. Two compounds (**3c**) and (**7c**) exhibited slight target selectivity by IC_{50} = 0.367 and IC_{50} = 0.0864 μM inhibitory data. The dihydroxy phenyl derivative (**7b**) is considered the most potent glycogen phosphorylase inhibitor by IC_{50} = 0.01372 μM. In contrast the benzylamine derivative (**3e**) showed less potency against this target by IC_{50} = 0.262 μM (Figure 2B).

2.2.3. In Vivo Antidiabetic Screening

The compound (**7b**) was tested on Sprague-Dawley (SD) rats for the effect on the blood glucose level, as described in the experimental Section 3.8, and the results are reported in (Table 2) and (Figure 3). Blood glucose levels were measured after fasting for 15 h (fasting reading), followed by the administration of a 5-mg meal (reading 1). Moreover, a second day reading after treatment with normal saline, acarbose, or (**7b**) compound blood glucose level (reading 2) followed by a 5-mg meal, was measured. It was shown that diabetic rats exhibited an increase in blood glucose level to above 200 mg/dL. In addition, the blood glucose level after 15 h fasting followed by a meal of 5 mg (reading 1) was compared to the blood glucose levels under the same conditions, and following the administration of normal saline, acarbose or compound (**7b**). For the control non-diabetic non-treated group and the diabetic non- treated group, no significant difference between (readings 1 and 2) was shown. For the group of rats treated with acarbose or compound (**7b**) one hour before a meal, blood glucose levels decreased from 147 ± 2 to 136 ± 3.28 and 120 ± 0.88 mg/dL to 116 ± 0.57, respectively. Finally, the target compound (**7b**) succeeded in decreasing the blood glucose level of diabetic rats better than the reference oral antidiabetic drug, acarbose.

Table 2. In vivo blood glucose data.

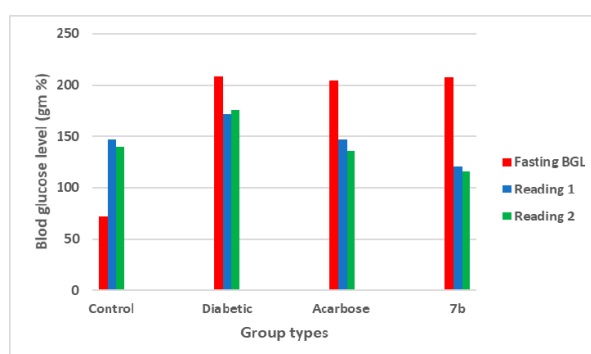| Groups	Blood Glucose Level (mg/dL)		
	Fasting	Reading 1	Reading 2
Control	72 ± 1.72	147 ± 0.88	140 ± 3.17
Diabetic	209 ± 0.66	172 ± 2.72	176 ± 2.90
Acarbose	204 ± 4.5	147 ± 2.0	136 ± 3.28
7b	207 ± 0.88	120 ± 0.88	116 ± 0.57

Figure 3. The bar chart of the effect of reference drug and target compound (**7b**) on the blood glucose level in treated and non-treated rats.

2.3. Molecular Docking Studies and SAR Analyses

To rationalize the experimental results obtained, molecular docking studies were accomplished on representative compounds (**5b**) and (**7b**) against the glycogen phosphorylase site structure (Figure 4A). The results are presented in (Figure 4) and (Table 3). It was clear that all compound fragments share in the interaction with the binding pockets. This means the activity of such series are related to both scaffold and terminal fragments. Two compounds of sulfonamide and benzylidine substructures that constitute most anti-glycogen phosphorylase inhibitors were docked and compared to the bound ligand, GSK254. From the data reported, compound GSK254 showed two stable hydrogen bonding interactions between Arg310 with a terminal carboxylic group. Moreover, the anthranilate C=O scaffold formed a stable hydrogen bond with the amino acid Gln71. In addition, the compound is stabilized by an extra hydrophobic interaction with Ile68 through the phenyl fragment (Figure 4B). The behavior of compound (**7b**) as a potent inhibitor in the binding pocket showed three consistently stable hydrogen bonds with the terminal hydroxyl groups, carbonyl linker, and pyridine part with corresponding amino acid residues Asp76, Tyr738 and Gln71 (Figure 4C). All the modeled drugs displayed hydrophobic interactions that stabilized the compounds in the binding pockets via the terminal pyridyl and anthranilate ring with Gln71, Ile68, Phe196, or Arg193 residues. With regards to compound (**5b**), two stable hydrogen bonds were formed with the pocket residues Gln71 and Arg193 through the pyridine ring and anthranilate carbonyl function linker (Figure 4D). The scaffold, linker, and terminal fragments are essential for activity and it is very important to take care during any optimization processes.

Table 3. Docking data of selected target compounds.

Compounds	Fragment	Target Residues (Distance, Å)	Interaction	Binding Energy (dG)
5b	C=O (anthranilate)	Gln71 (3.14)	H-bonding	−14.5
	Phenyl (sulphonamide)	Tyr75, Gln71, Gln72	Hydrophobic	
	Pyridine	Arg193 (3.08)	H-bonding	
		Ile68	Hydrophobic	
	Phenyl (anthranilate)	Ala313	Aromatic stacking	
7b	–OH	Asp76 (3.1)	H-bonding	−15.4
	–OH	Tyr738 (4.65)	H-bonding	
	C=O (anthranilate)	Gln71 (3.05)	H-bonding	
	Pyridine	Phe196	Hydrophobic	
	Phenyl (anthranilate)	Ile68	Hydrophobic	
GSK254	Carboxylic gp.	Arg310 (2.89)	H-bonding	−13.5
	Phenyl (anthranilate)	Ile68	Hydrophobic	
	Carbonyl linker	Gln71 (3.08)	H-bonding	

The data reported in the table are extracted from MOE program, Chemical Computing Group, (Montreal, QC, Canada) showing the corresponding amino acid residues in the enzyme pocket, corresponding fragments of ligands, interaction distances, types of interaction, and their binding energy to some selected drugs.
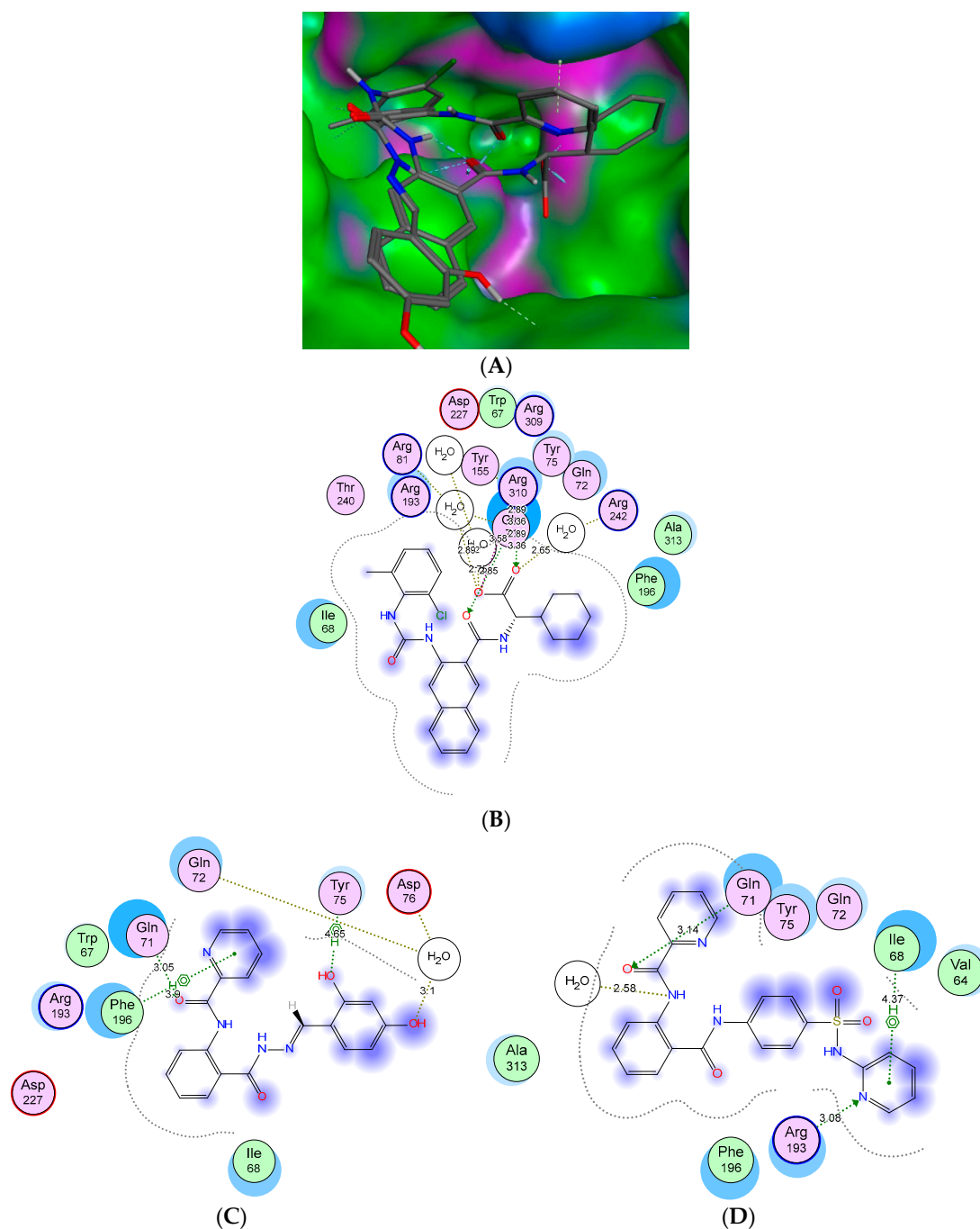
Figure 4. Docking of selected compounds (**7b**) and (**5b**) with glycogen phosphorylase protein target, PDB (3DD1). 3D and 2D interaction graphs are reported for (**A**) 3D target structure; (**B**) bound drug; GSK254, (**C**) (**7b**) and (**D**) (**5b**).

3. Materials and Methods

3.1. Chemistry

Infrared spectra were obtained using a schimadzu FT-IR 8201 PC, spectrophotometer (Kyoto, Japan). [1]H and ^{13}C neuclear magnetic resonance (NMR) spectra were obtained using a Bruker AC 400 NMR spectrometer (Billerica, MA, USA) at 400 and 100 MHz, respectively. All ^{1}H and ^{13}C nuclear magnetic resonance (NMR) spectral results are recorded as chemical shifts (d) relative to the

internal transcranial magnetic stimulation (TMS). Microanalysis was performed by Chemical and Micro-Analytical Services (CMAS), (Highton, VIC, Australia). Melting point determinations were carried out using a Stuart Scientific (SMP3) melting point apparatus (Staffordshire, UK) and all melting points are uncorrected. Reaction courses and product mixtures were routinely monitored by thin-layer chromatography (TLC) on silica gel pre-coated F_{254} Merck plates (Darmstadt, Germany).

Starting Materials:

The starting reagents, methyl 2-aminobenzoate, picolinoyl chloride, cesium carbonate, triethylamine, dimethylformamide (DMF), acetonitrile, substituted benzylamine, substituted sulphonamide, potassium tert-butoxide, hydrazine hydrate and substituted aryl aldehyde were purchased from Sigma-Aldrich (St. Louis, MO, USA) and were used as received.

3.2. Synthesis and Characterization of Methyl 2-(Picolinamido)benzoate (1)

According to our previously reported method [32], product **1** was prepared in 82% yield from the reaction of methyl-2-aminobenzoate (1 mmol) and triethylamine (5 mmol) in dry DMF (10 mL), 2-pyridinecarbonyl chloride (1.2 mmol) was then added drop wise. The reaction mixture was heated under reflux for 4 h. After cooling, the reaction mixture was poured into ice water and the formed solid was collected by filtration and recrystallized from ethanol to give (**1**), mp 210–212 °C. νmax (KBr)/cm^{-1} 3358, 2955 (N-H), 1710 (C=O), 1698 (C=O); ^{1}H NMR (DMSO-d_6) δ 11.5 (s, 1H, NHCO), 8.6–7.2 (m, 8H, Ph-H and pyridyl-H), 3.1 (s, 3H, O–CH$_3$); ^{13}C NMR (DMSO-d_6) δ 168.8, 162.2, 147.7, 140.2, 137.6, 133.7, 130.6, 126.6, 124.0, 122.6, 122.3, 119.5, 116.3 (Ar-C, C=O), 53.1 (CH$_2$); Found: C, 65.65; H, 4.79; N, 10.91; $C_{14}H_{12}N_2O_3$ requires C, 65.62; H, 4.72; N, 10.93.

3.3. General Procedure for the Synthesis of Diamides 3a–e and 5a–c

In slight modification to our previous reported method to obtain better yields of compounds **3a–e** and **5a–c**, [32] a mixture of the appropriate benzylamine and/or sulfonamide derivatives (1.5 mmol), potassium tert-butoxide (6.5 mmol) in acetonitrile (10 mL) was stirred under reflux for two hours, a solution of methyl 2-(picolinamido)benzoate (**1**) (1 mmol) in acetonitrile (10 mL) was added portion-wise. The reaction mixture was refluxed for overnight until the reaction was judged complete by TLC and then poured into ice water. The resulting solid thus formed was filtered and recrystallized from the appropriate solvent.

N-(2-(Benzylcarbamoyl)phenyl)picolinamide (**3a**). This compound was obtained in 92% yield (from ethanol), mp 241–242 °C. νmax (KBr)/cm^{-1} 3278, 2895 (N-H), 1704 (C=O), 1671 (C=O); ^{1}H NMR (DMSO-d_6) δ 11.2 (s, 1H, NHCO), 9.3 (s, 1H, NHCH$_2$), 8.9–7.2 (m, 13H, Ph-H, pyridyl-H and benzyl-H), 3.8 (s, 2H, CH$_2$); ^{13}C NMR (DMSO-d_6) δ 167.8, 162.7, 152.1, 138.1, 137.9, 137.2, 132.6, 131.7, 128.5, 128.4, 127.0, 126.9, 126.8, 126.5, 124.5, 122.6, 115.3, 122.2, 119.4 (Ar-C, C=O), 44.1 (CH$_2$); Found: C, 72.50; H, 5.20; N, 12.69; $C_{20}H_{17}N_3O_2$ requires C, 72.49; H, 5.17; N, 12.68.

N-(2-((4-Methoxybenzyl)carbamoyl)phenyl)picolinamide (**3b**). This compound was obtained in 93% yield (from ethanol), mp 225–227 °C. νmax (KBr)/cm^{-1} 3368, 2965 (N-H), 1715 (C=O), 1695 (C=O); ^{1}H NMR (DMSO-d_6) δ 10.6 (s, 1H, NHCO), 9.2 (s, 1H, NHCH$_2$) 8.8–6.6 (m, 12H, Ph-H, pyridyl-H and benzyl-H), 3.8 (s, 2H, CH$_2$), 3.8 (s, 3H, O-CH$_3$); ^{13}C NMR (DMSO-d_6) δ 167.8, 162.6, 158.6, 151.2, 147.8, 137.9, 137.6, 132.3, 131.6, 130.7, 13.5, 130.2, 126.4, 125.0, 124.6, 122.3, 119.5, 114.2, 114.1 (Ar-C, C=O), 55.8 (OCH$_3$), 44.1 (CH$_2$); Found: C, 69.76; H, 5.27; N, 11.59; $C_{21}H_{19}N_3O_3$ requires C, 69.79; H, 5.30; N, 11.63.

N-(2-((4-Fluorobenzyl)carbamoyl)phenyl)picolinamide (**3c**). This compound was obtained in 85% yield (from ethanol), mp 240–242 °C. νmax (KBr)/cm^{-1} 3358, 2955 (N-H), 1725 (C=O), 1695 (C=O); ^{1}H NMR (DMSO-d_6) δ 10.5 (bs, 1H, NHCO), 9.3 (bs, 1H, NHCH$_2$), 8.2–7.1 (m, 12H, Ph-H, pyridyl-H and benzyl-H), 3.9 (s, 2H, CH$_2$); ^{13}C NMR (DMSO-d_6) δ 167.8, 162.7, 160.9, 151.3, 147.9, 137.9, 137.5, 133.2, 132.3, 131.6, 128.5, 128.4, 126.3, 125.0, 124.7, 122.3, 119.1, 115.4, 114.7 (Ar-C, C=O), 44.2 (CH$_2$); Found: C, 68.76; H, 4.67; N, 12.75; $C_{20}H_{16}FN_3O_2$ requires C, 68.76; H, 4.62; N, 12.03.

N-(2-((4-Chlorobenzyl)carbamoyl)phenyl)picolinamide (**3d**). This compound was obtained in 82% yield (from ethanol), mp 233–235 °C. νmax (KBr)/cm^{-1} 3358, 2955 (N-H), 1710 (C=O), 1698 (C=O); ^{1}H NMR (DMSO-d_6) δ 10.6 (s, 1H, NHCO), 8.9 (s, 1H, NHCH$_2$), 8.5–6.9 (m, 12H, Ph-H, pyridyl-H and benzyl-H), 3.9 (s, 2H, CH$_2$); ^{13}C NMR (DMSO-d_6) δ 167.8, 162.7, 151.3, 147.2, 137.9, 137.5, 136.0, 134.7, 134.6, 133.2, 132.3, 131.6, 128.6, 128.4, 126.8, 125.0, 124.4, 122.1, 119.4 (Ar-C, C=O), 44.4 (CH$_2$); Found: C, 65.66; H, 4.47; N, 11.47; C$_{20}$H$_{16}$ClN$_3$O$_2$ requires C, 65.67; H, 4.41; N, 11.49.

N-(2-((4-Methylbenzyl)carbamoyl)phenyl)picolinamide (**3e**). This compound was obtained in 80% yield (from ethanol), mp 275–278 °C. νmax (KBr)/cm^{-1} 3358, 2955 (N-H), 1713 (C=O), 1688 (C=O); ^{1}H NMR (DMSO-d_6) δ 10.5 (bs, 1H, NHCO), 9.2 (bs, 1H, NHCH$_2$), 8.4–6.9 (m, 12H, Ph-H, pyridyl-H and benzyl-H), 4.0 (s, 2H, CH$_2$), 2.3 (s, 3H, CH$_3$); ^{13}C NMR (DMSO-d_6) δ 167.8, 162.7, 152.3, 147.2, 138.0, 137.5, 136.3, 134.2, 132.3, 131.6, 129.0, 128.9, 128.1, 128.0, 126.4, 125.5, 124.9, 122.8, 119.1 (Ar-C, C=O), 44.5 (CH$_2$), 21.5 (CH$_3$); Found: C, 73.05; H, 5.57; N, 12.17; C$_{21}$H$_{19}$N$_3$O$_2$ C, 73.03; H, 5.54; N, 12.17.

N-(2-((4-Sulfamoylphenyl)carbamoyl)phenyl)picolinamide (**5a**). This compound was obtained in 85% yield (from 1,4-dioxane), mp 188–189 °C. νmax (KBr)/cm^{-1} 3357, 3203 (N-H), 1678 (C=O), 1632 (C=O), 1341, 1152 (S=O); ^{1}H NMR (DMSO-d_6) δ 11.5 (s, 1H, NHCO), 10.2 (s, 1H, NHCO), 8.6–6.7 (m, 12H, Ph-H, pyridyl-H and aminosulphonyl ph-H), 3.4 (bs, 2H, NH$_2$); ^{13}C NMR (DMSO-d_6) δ 167.2, 162.9, 151.2, 147.5, 141.3, 137.6, 137.2, 136.5, 132.6, 129.6, 129.4, 127.7, 126.5, 124.5, 123.2, 122.5, 119.6, 118.2, 118.0 (Ar-C, C=O); Found: C, 57.57; H, 4.09; N, 14.11; C$_{18}$H$_{15}$N$_3$O$_5$S requires C, 57.57; H, 4.07; N, 14.13.

N-(2-((4-(N-(Pyridin-2-yl)sulfamoyl)phenyl)carbamoyl)phenyl)picolinamide (**5b**). This compound was obtained in 83% yield (from acetonitraile), mp 209–211 °C. νmax (KBr)/cm^{-1} 3357, 3203 (N-H), 1675 (C=O), 1640 (C=O), 1341, 1152 (S=O); ^{1}H NMR (DMSO-d_6) δ 11.3 (s, 1H, NHCO), 10.8 (s, 1H, SO$_2$NH), 10.5 (s, 1H, NHCO), 8.6–6.7 (m, 16H, Ph-H, pyridyl-H and aminosulphonyl ph-H, pyridinyl-H); ^{13}C NMR (DMSO-d_6) δ 167.5, 162.4, 152.4, 151.5, 148.2, 147.4, 141.2, 139.1, 137.9, 137.5, 135.3, 132.6, 129.4, 129.7, 127.9, 126.3, 124.6, 123.4, 122.5, 119.5, 118.2, 118.0, 117.4, 109.5 (Ar-C, C=O); Found: C, 60.90; H, 4.05; N, 14.80; C$_{24}$H$_{19}$N$_5$O$_4$S requires C, 60.88; H, 4.04; N, 14.79.

N-(2-((4-(N-(Thiazol-2-yl)sulfamoyl)phenyl)carbamoyl)phenyl)picolinamide (**5c**). This compound was obtained in 74% yield (from ethanol), mp 217–219 °C. νmax (KBr)/cm^{-1} 3348, 3205 (N-H), 1681 (C=O), 1642 (C=O), 1341, 1152 (S=O); ^{1}H NMR (DMSO-d_6) δ 11.2 (s, 1H, NHCO), 10.8 (s, 1H, SO$_2$NH), 10.3 (bs, 1H, NHCO), 8.6–6.3 (m, 14H, Ph-H, pyridyl-H and aminosulphonyl ph-H, thiazole-H); ^{13}C NMR (DMSO-d_6) δ 171.6, 167.3, 162.7, 151.4, 147.9, 141.7, 137.9, 137.5, 137.0, 136.8, 134.9, 132.8, 129.4, 128.9, 127.2, 126.7, 124.5, 123.2, 122.7, 119.5, 118.4, 118.0, 112.1 (Ar-C, C=O); Found: C, 55.09; H, 3.59 N, 14.58; C$_{22}$H$_{17}$N$_5$O$_4$S$_2$ requires C, 55.10; H, 3.57; N, 14.60.

3.4. Synthesis and Characterization of N-(2-(Hydrazinecarbonyl)phenyl)picolinamide (6)

A mixture of methyl 2-(picolinamido)benzoate (**1**) (1 mmol) and hydrazine hydrate (5 mmol) in ethanol (20 ml) was refluxed for 8 h. After cooling, the mixture was poured into crushed ice and the formed solid was filtered off. The crude product was recrystallized from hot water to give compound (**6**) in 95% yield, mp 210–212 °C. νmax (KBr)/cm^{-1} 3204–3210 (NH$_2$, NH), 1689 (C=O), 1657 (C=O); ^{1}H NMR (DMSO-d_6) δ 12.4 (s, 1H, NHNH$_2$), 10.2 (s, 1H, NHCO), 8.6–6.7 (m, 7H, ArH, Ph-H and pyridyl-H), 4.7 (s, 2H, NH$_2$); ^{13}C NMR (DMSO-d_6) δ 164.0, 162.6, 151.1, 147.7, 138.0, 137.8, 132.5, 127.3, 126.4, 124.5, 123.7, 122.6, 119.5 (Ar-C, C=O); Found: C, 60.90; H, 4.70; N, 21.88; C$_{13}$H$_{12}$N$_4$O$_2$ requires C, 60.93; H, 4.72; N, 21.86.

3.5. General Procedure for the Synthesis of Schiff Bases-Type Hydrazones 7a–d

In slight modification to our previous reported method to obtain better yields of compounds **7a–d** [32] a mixture of *N*-(2-(hydrazinecarbonyl)phenyl)picolinamide (**6**) (1 mmol) and the appropriate aromatic aldehyde (1 mmol) in 20 mL of ethanol and few drops of HCl was refluxed for 3 h.

After cooling, the reaction mixture was poured into ice water, and the formed solid product was filtered. The crude product was recrystallized from the appropriate solvent.

(E)-N-(2-(2-Benzylidenehydrazine-1-carbonyl)phenyl)picolinamide (**7a**). This compound was obtained in 83% yield (from ethanol), mp 205–207 °C. νmax (KBr)/cm^{-1} 3248, 2895 (N-H), 1697 (C=O), 1676 (C=O), 1621 (N=N); ^{1}H NMR (DMSO-d_6) δ 11.7 (s, 1H, CONH), 11.3 (s, 1H, CONH), 8.5–6.7 (m, 14H, Ph-H, pyridyl-H, phenyl-H and H-C=N); ^{13}C NMR (DMSO-d_6) δ 165.6, 162.4, 151.8, 147.2, 146.8, 137.9, 137.6, 133.4, 132.6, 131.1, 130.0, 129.7, 128.4, 128.0, 127.4, 126.7, 124.7, 123.6, 122.5, 119.4; (Ar-C, C=O, C=N); Found: C, 69.75; H, 4.66; N, 16.26; $C_{20}H_{16}N_4O_2$ requires C, 69.76; H, 4.68; N, 16.27.

(E)-N-(2-(2-(2,4-Dihydroxybenzylidene)hydrazine-1-carbonyl)phenyl)picolinamide (**7b**). This compound was obtained in 81% yield (from ethanol), mp 215–217 °C. νmax (KBr)/cm^{-1} 3380–3252 (O-H), 3248, 2895 (N-H), 1697 (C=O), 1676 (C=O), 1597 (N=N); ^{1}H NMR (DMSO-d_6) δ 11.8 (s, 1H, CONH), 10.5 (s, 1H, CONH), 9.3 (bs, 1H, OH), 8.6–6.4 (m, 13H, Ph-H, pyridyl-H, phenyl-H, and H-C=N, OH-H); ^{13}C NMR (DMSO-d_6) δ 165.1, 162.4, 162.0, 161.7, 151.5, 147.2, 146.5, 137.9, 137.7, 133.5, 132.7, 127.5, 126.4, 124.5, 123.3, 122.4, 119.6, 112.5, 109.5, 103.7 (Ar-C, C=O, C=N); Found: C, 63.81; H, 4.33; N, 14.87; $C_{20}H_{16}N_4O_4$ requires C, 63.83; H, 4.29; N, 14.89.

(E)-N-(2-(2-(Pyridin-2-ylmethylene)hydrazine-1-carbonyl)phenyl)picolinamide (**7c**). This compound was obtained in 80% yield (from ethyl acetate), mp 225–227 °C. νmax (KBr)/cm^{-1} 3238, 2905 (N-H), 1705 (C=O), 1667 (C=O), 1620 (N=N); ^{1}H NMR (DMSO-d_6) δ 12.3 (s, 1H, CONH), 11.7 (s, 1H, CONH), 8.6–6.7 (m, 13H, Ph-H, pyridyl-H, H-C=N and pyridyl-H); ^{13}C NMR (DMSO-d_6) δ 165.4, 162.2, 153.3, 151.5, 149.7, 147.7, 144.6, 137.9, 137.5, 136.2, 132.3, 127.9, 127.1, 126.2, 124.8, 123.5, 122.4, 120.1, 119.4 (Ar-C, C=O, C=N); Found: C, 66.09; H, 4.35; N, 20.29; $C_{19}H_{15}N_5O_2$ requires C, 66.08; H, 4.38; N, 20.28.

(E)-N-(2-(2-(2,4-Dichlorobenzylidene)hydrazine-1-carbonyl)phenyl)picolinamide (**7d**). This compound was obtained in 75% yield (from toluene), mp 212–214 °C. νmax (KBr)/cm^{-1} 3248, 2895 (N-H), 1697 (C=O), 1676 (C=O), 1597 (N=N); ^{1}H NMR (DMSO-d_6) δ 11.8 (s, 1H, CONH), 11.3 (s, 1H, CONH), 8.6–6.4 (m, 12H, ArH, Ph-H, pyridyl-H, phenyl-H, and H-C=N); ^{13}C NMR (DMSO-d_6) δ 165.4, 162.6, 151.1, 147.2, 138.7, 137.9, 137.3, 132.8, 132.4, 131.0, 129.5, 129.0, 128.3, 127.7, 127.3, 126.8, 124.6, 123.2, 122.1, 119.4 (Ar-C, C=O, C=N); Found: C, 58.11; H, 3.40; N, 13.54; $C_{20}H_{14}Cl_2N_4O_2$ requires C, 58.13; H, 3.41; N, 13.56.

3.6. α-Glucosidase Inhibition Assay

α-Glucosidase inhibition assay was performed spectrophotometrically. α-Glucosidase from *Saccharomyces cerevisiae* (Abcam, Cambridge, UK) was dissolved in phosphate buffer (pH 6.8, 50 mM). Test compounds were dissolved in DMSO. In 96-well microtiter plates, 20 µL of test sample, 20 µL of enzyme (20 mU/mL) and 135 µL of buffer were added and incubated for 15 minutes at 37 °C. After incubation, 25 µL of *p*-nitrophenyl-α-D-glucopyranoside (2 mM, Abcam) was added and change in absorbance was monitored for 20 min at 400 nm. Test compound was replaced by DMSO (10% final) as control. Deoxynojirimycin hydrochloride (Abcam) was used as a standard inhibitor. The assays were done in triplicate. IC$_{50}$ values were calculated from non-linear regression curve of percentage inhibition versus log compound concentration.

3.7. Glycogen Phosphorylase Enzyme Assay

Rabbit muscle glycogen phosphorylase a (from Abcam, 0.475 mg/ mL) activity was measured in the direction of glycogen synthesis by the release of phosphate from glucose-1-phosphate using a 384-well plate at 22 °C in 45 mL of buffer containing 50 mM Hepes (pH 7.2), 100 mM KCl, 2.5 mM EGTA, 2.5 Mm MgCl$_2$, 0.25 Mm glucose-1-phosphate, and 1 mg/mL glycogen with a 30-min incubation time. Phosphate was measured at 620 nm, 5 minutes after the addition of 150 mL of 1 MHCl containing 10 mg/mL ammonium molybdate and 0.38 mg/mL malachite green. Test compounds were added to

the assay in 5 mL of 14% DMSO. Compounds were tested against a deoxynojirimycin hydrochloride (Abcam) standard in 11 point concentration response curve in duplicate on two separate occasions. Data were analyzed using GraphPad Prism v.4.03, GraphPad Software, (La Jolla, CA, USA).

A nonlinear regression (curve fit) analysis with a sigmoidal dose response equation (variable slope) was applied to generate IC_{50} and hill slope values. The reported IC_{50} had a hill slope between 0.7 and 1.2 and a Z0 value of ~0.8. Compounds were screened with maximal concentrations of 222 mM. The assay was carefully monitored for signs of compound insolubility. The results are presented as mean values from three determinations.

3.8. In Vivo Antidiabetic Screening

Twenty male Sprague–Dawley (SD) rats were maintained in an air-conditioned room (25 °C) at a constant humidity (55–60%). All rats were provided with a standard rat diet containing 60% carbohydrate (*w/w*), 2% fat (*w/w*), 17.5% protein (*w/w*), 8% fiber (*w/w*), and water ad libitum. The experiments were performed in accordance with the internationally accepted standard ethical guidelines for laboratory animal use and care, as described in the European Community guidelines. The Institutional Animal Ethics Committee of Al-Azhar University approved the study protocols (approval No: 409/432, 3/2018). Diabetes was induced in 12 Sprague–Dawley (SD) male rats by a single intraperitoneal injection of 40 mg/kg streptozocin (STZ) dissolved in 0.1 M/L citrate buffer at a pH of 4.5. Three rats were injected with normal saline and vehicle only to serve as negative controls. The remaining diabetic rats (nine) were identified by an increase in blood glucose more than 200 ± 10 mg/dL after one week. Blood glucose levels were measured using One Touch Ultra 2 glucometer (Lifescan inc., Wayne, USA) every week for the following two weeks to confirm the diabetic status. Rats were 6–8 weeks of age and the average weight when starting the experiment was 200 ± 20 g. Twelve rats were randomly assigned to four groups. Group 1: non-diabetic non-treated (control). Group 2: Diabetic non-treated. Group 3: Diabetic and administrated acarbose before meals. Group 4: Diabetic and administrated our new compound before a meal. Briefly; the first group was injected with an IP vehicle only. The other three groups were injected with streptozocin (STZ) and developed diabetes. The second group was diabetic and untreated. The third group was diabetic rats treated with acarbose at 40 mg per 100 g body weight 30 min. before meal using oral tube. The fourth group administrated 40 mg/100 g body weight of the test compound (**7b**). Rats were fasted over 15 h and blood sugar levels were measured (pretreatment). For each rat, 5 mg standard rat diet was supplied to each rat and blood glucose levels were measured to detect increases after 1 h. Rats were fed again with the same amount after 8 h. Food was removed to allow animals to fast again for 15 h. On the following day, groups 1 and two were not given any treatment, while group 3 rats were given acarbose (positive control) and group 4 were given the test compound (**7b**). Blood glucose levels were measured in tail vein blood samples taken from fasting rats (time point 0), then designated groups are fed either acarbose or the test compound, suspended in PBS and delivered using an oral tube. After half an hour, the rats were given five mg. Blood samples were taken after 1 h. Blood glucose was expected to rise after meal and the effect of the drugs was evaluated according to their abilities to control post-meal excursions.

3.9. Molecular Docking

Molecular docking simulation was done for the selected potent target compounds into the three-dimensional complex of the biological target including the crystal structure of glycogen phosphorylase (PDB code: 3DD1) at 2.6 Å resolution focusing on the AMP site [39] was carried out using the AutoDock software package (version 4.0) (La Julla, California, USA) as implemented through the graphical user interface AutoDock Tools (ADT) [40]. Prior to the calculations, crystallographic water and ligand molecules were removed from the X-ray structure. Hydrogen atoms were added to the structure with the molecular operating environment (MOE, 2012) (2012) [41] and atomic partial charges were calculated using AutoDock Tools. Selected active anthranilate compounds were docked

into the active site of the target to predict compound binding mode. For flexible docking, AutoDock standard parameter settings were applied. High-scoring binding poses were selected on the basis of visual inspection.

4. Conclusions

A series of *N*-pyridyl anthranilate derivatives were designed, synthesized, and tested for screening of their inhibitory activity against two promising antidiabetic α-glucosidase and glycogen phosphorylase targets. The design of such compounds involves hybrids of benzylamine, sulfonamides and benzylidine fragments linked to the acidic part of the anathranilic acid scaffold. Most of the tested diamide compounds exhibited potent α-glucosidase and glycogen phosphorylase inhibitory effect with nanomolar concentrations. The most effective derivatives are (**5b**) and (**7b**) with terminal sulfapyridine and dihydroxy substituted phenyl fragments. Furthermore, the most active compound (**7b**), was tested for decreasing blood glucose level, and the data proved that these novel compounds could decrease the elevated abnormal glucose level better than the reference drug. Extensive molecular docking studies were applied for an investigation of the structure–activity relationship of these compounds. It is anticipated that new inhibitors developed using these techniques will soon be seen in the clinic as effective antidiabetic drugs.

References

1. Nyenwe, E.A.; Jerkins, T.W.; Umpierrez, G.E.; Kitabchi, A.E. Management of type 2 diabetes: Evolving strategies for the treatment of patients with type 2 diabetes. *Metab. Clin. Exp.* **2011**, *60*, 1–23. [CrossRef] [PubMed]
2. Xie, Y.; Xie, Z. Chapter 7—Treatment of Diabetic Cardiomyopathy through Upregulating Autophagy by Stimulating AMP-Activated Protein Kinase A2—Hayat, M.A. In *Autophagy: Cancer, Other Pathologies, Inflammation, Immunity, Infection, and Aging*; Academic Press: Amsterdam, The Netherlands, 2014; pp. 91–103.
3. American Diabetes Association. Diagnosis and Classification of Diabetes Mellitus. *Diabetes Care* **2009**, *32* (Suppl. 1), S62–S67.
4. Reinehr, T.; Schober, E.; Roth, C.L.; Wiegand, S.; Holl, R. Type 2 diabetes in children and adolescents in a 2-year follow-up: Insufficient adherence to diabetes centers. *Horm. Res.* **2008**, *69*, 107–113. [CrossRef] [PubMed]
5. Weiss, R.; Taksali, S.E.; Caprio, S. Development of type 2 diabetes in children and adolescents. *Curr. Diabetes Rep.* **2006**, *6*, 182–187. [CrossRef]
6. WHO. Cardiovascular Diseases. 2017. Available online: http://www.who.int/mediacentre/factsheets/fs317/en/ (accessed on 15 May 2017).
7. Jahan, H.; Choudhary, M.I. Glycation, carbonyl stress and AGEs inhibitors: A patent review. *Expert Opin. Ther. Pat.* **2015**, *25*, 1267–1284. [PubMed]
8. Asif, M. The prevention and control the type-2 diabetes by changing lifestyle and dietary pattern. *J. Educ. Health Promot.* **2014**, *3*, 1. [CrossRef] [PubMed]
9. Zhang, N.; Du, S.M.; Ma, G.S. Current lifestyle factors that increase risk of T2DM in China. *Eur. J. Clin. Nutr.* **2017**, *71*, 832. [CrossRef] [PubMed]
10. Hu, F.B. Globalization of Diabetes: The role of diet, lifestyle, and genes. *Diabetes Care* **2011**, *34*, 1249–1257. [CrossRef] [PubMed]
11. WHO. Biological, Behavioural and Contextual Rationale. 2014. Available online: http://www.who.int/elena/titles/bbc/fruit_vegetables_ncds/en/ (accessed on 15 May 2017).
12. Prentki, M.; Nolan, C.J. Islet beta cell failure in type 2 diabetes. *J. Clin. Investig.* **2006**, *116*, 1802–1812. [CrossRef] [PubMed]

13. Kahn, S.E.; Haffner, S.M.; Heise, M.A.; Herman, W.H.; Holman, R.R.; Jones, N.P.; Kravitz, B.G.; Lachin, J.M.; O'Neill, M.C.; Zinman, B.; et al. Glycemic durability of rosiglitazone, metformin, or glyburide monotherapy. *N. Engl. J. Med.* **2006**, *355*, 2427–2443. [CrossRef] [PubMed]

14. Monami, M.; Lamanna, C.; Marchionni, N.; Mannucci, E. Comparison of different drugs as add-on treatments to metformin in type 2 diabetes: A meta-analysis. *Diabetes Res. Clin. Pract.* **2008**, *79*, 196–203. [CrossRef] [PubMed]

15. Miller, B.R.; Nguyen, H.; Hu, C.J.-H.; Lin, C.; Nguyen, Q.T. New and Emerging Drugs and Targets for Type 2 Diabetes: Reviewing the Evidence. *Am. Health Drug Benefits* **2014**, *7*, 452–463. [PubMed]

16. Woerle, H.J.; Szoke, E.; Meyer, C.; Dostou, J.M.; Wittlin, S.D.; Gosmanov, N.R.; Welle, S.L.; Gerich, J.E. Mechanisms for abnormal postprandial glucose metabolism in type 2 diabetes. *Am. J. Physiol. Endocrinol. Metab.* **2006**, *290*, E67–E77. [CrossRef] [PubMed]

17. Magnusson, I.; Rothman, D.L.; Katz, L.D.; Shulman, R.G.; Shulman, G.I. Increased rate of gluconeogenesis in type II diabetes mellitus. A 13C nuclear magnetic resonance study. *J. Clin. Investig.* **1992**, *90*, 1323–1327. [CrossRef] [PubMed]

18. Chen, J.; Gong, Y.; Liu, J.; Hua, W.; Zhang, L.; Sun, H. Synthesis and biological evaluation of novel pyrazolo[4,3-b]oleanane derivatives as inhibitors of glycogen phosphorylase. *Chem. Biodivers.* **2008**, *5*, 1304–1312. [CrossRef] [PubMed]

19. Liu, J.; Zhang, H.; Zhu, P.; Wu, X.; Yao, H.; Ye, W.; Jiang, J.; Xu, J. Synthesis and biological evaluation of ambradiolic acid as an inhibitor of glycogen phosphorylase. *Fitoterapia* **2015**, *100*, 50–55. [CrossRef] [PubMed]

20. Zhang, P.; Hao, J.; Liu, J.; Lu, Q.; Sheng, H.; Zhang, L.; Sun, H. Synthesis of 3-deoxypentacyclic triterpene derivatives as inhibitors of glycogen phosphorylase. *J. Nat. Prod.* **2009**, *72*, 1414–1418. [CrossRef] [PubMed]

21. Borges de Melo, E.; da Silveira Gomes, A.; Carvalho, I. α- and β-Glucosidase inhibitors: Chemical structure and biological activity. *Tetrahedron* **2006**, *62*, 10277–10302. [CrossRef]

22. Derosa, G.; Maffioli, P. α-Glucosidase inhibitors and their use in clinical practice. *Arch. Med. Sci. AMS* **2012**, *8*, 899–906. [CrossRef] [PubMed]

23. Suleiman, M.M.; Isaev, S.G.; Klenina, O.V.; Ogurtsov, V.V. Synthesis, biological activity evaluation and QSAR studies of novel 3-(aminooxalyl-amino)-and 3-(carbamoylpropionylamino)-2-phenylamino-benzoic acid derivatives. *J. Chem. Pharm. Res.* **2014**, *6*, 1219–1235.

24. Thongtan, J.; Saenboonrueng, J.; Rachtawee, P.; Isaka, M. An antimalarial tetrapeptide from the entomopathogenic fungus Hirsutella sp. BCC 1528. *J. Nat. Prod.* **2006**, *69*, 713–714. [CrossRef] [PubMed]

25. De Luca, S.; Saviano, M.; Lassiani, L.; Yannakopoulou, K.; Stefanidou, P.; Aloj, L.; Morelli, G.; Varnavas, A. Anthranilic acid based CCK1 receptor antagonists and CCK-8 have a common step in their "receptor desmodynamic processes". *J. Med. Chem.* **2006**, *49*, 2456–2462. [CrossRef] [PubMed]

26. Tiwari, D.; Haque, S.; Misra, S.; Chandra, R. Synthesis and pharmacological screening of Nsubstituted anthranilic acid derivatives. *Int. J. Dev. Res.* **2011**, *3*, 265–271.

27. Tzin, V.; Galili, G. The Biosynthetic Pathways for Shikimate and Aromatic Amino Acids in Arabidopsis thaliana. *Arabidopsis Book/Am. Soc. Plant Biol.* **2010**, *8*, e0132.

28. Syed, M.M.; Parekh, A.B.; Tomita, T. Receptors involved in mechanical responses to catecholamines in the circular muscle of guinea-pig stomach treated with meclofenamate. *Br. J. Pharmacol.* **1990**, *101*, 809–814. [CrossRef] [PubMed]

29. Aboul-Fadl, T.; Abdel-Aziz, H.A.; Kadi, A.; Bari, A.; Ahmad, P.; Al-Samani, T.; Ng, S.W. Microwave-assisted one-step synthesis of fenamic acid hydrazides from the corresponding acids. *Molecules* **2011**, *16*, 3544–3551. [CrossRef] [PubMed]

30. Cocco, M.T.; Congiu, C.; Lilliu, V.; Onnis, V. Synthesis of new N-(2-(trifluoromethyl)pyridin-4-yl)anthranilic acid derivatives and their evaluation as anticancer agents. *Bioorg. Med. Chem. Lett.* **2004**, *14*, 5787–5791. [CrossRef] [PubMed]

31. Adeniji, A.O.; Twenter, B.M.; Byrns, M.C.; Jin, Y.; Winkler, J.D.; Penning, T.M. Discovery of substituted 3-(phenylamino)benzoic acids as potent and selective inhibitors of type 5 17β-hydroxysteroid dehydrogenase (AKR1C3). *Bioorg. Med. Chem. Lett.* **2011**, *21*, 1464–1468. [CrossRef] [PubMed]

32. Ihmaid, S.; Ahmed, H.E.A.; Zayed, M.F. The Design and Development of Potent Small Molecules as Anticancer Agents Targeting EGFR TK and Tubulin Polymerization. *Int. J. Mol. Sci.* **2018**, *19*, 408. [CrossRef] [PubMed]

33. Choudhary, M.I.; Cardellina, J.H.; Khan, K.M.; Atta, A. Anthranilic Acid Derivatives: Novel Inhibitors of Advanced Glycation end Products (AGES) Formation. U.S. Patent US20150051286A1, 15 August 2016.

34. Per, W.; Jan, B. The Chemistry of Anthranilic Acid. *Curr. Org. Synth.* **2006**, *3*, 379–402.

35. Thomson, S.A.; Banker, P.; Bickett, D.M.; Boucheron, J.A.; Carter, H.L.; Clancy, D.C.; Cooper, J.P.; Dickerson, S.H.; Garrido, D.M.; Nolte, R.T.; et al. Anthranilimide based glycogen phosphorylase inhibitors for the treatment of type 2 diabetes. Part 3: X-ray crystallographic characterization, core and urea optimization and in vivo efficacy. *Bioorg. Med. Chem. Lett.* **2009**, *19*, 1177–1182. [CrossRef] [PubMed]

36. Sparks, S.M.; Banker, P.; Bickett, D.M.; Carter, H.L.; Clancy, D.C.; Dickerson, S.H.; Dwornik, K.A.; Garrido, D.M.; Golden, P.L.; Nolte, R.T.; et al. Anthranilimide-based glycogen phosphorylase inhibitors for the treatment of type 2 diabetes: 1. Identification of 1-amino-1-cycloalkyl carboxylic acid headgroups. *Bioorg. Med. Chem. Lett.* **2009**, *19*, 976–980. [CrossRef] [PubMed]

37. Sparks, S.M.; Banker, P.; Bickett, D.M.; Clancy, D.C.; Dickerson, S.H.; Garrido, D.M.; Golden, P.L.; Peat, A.J.; Sheckler, L.R.; Tavares, F.X.; et al. Anthranilimide-based glycogen phosphorylase inhibitors for the treatment of Type 2 diabetes: 2. Optimization of serine and threonine ether amino acid residues. *Bioorg. Med. Chem. Lett.* **2009**, *19*, 981–985. [CrossRef] [PubMed]

38. Evans, K.A.; Li, Y.H.; Coppo, F.T.; Graybill, T.L.; Cichy-Knight, M.; Patel, M.; Gale, J.; Li, H.; Thrall, S.H.; Tew, D.; et al. Amino acid anthranilamide derivatives as a new class of glycogen phosphorylase inhibitors. *Bioorg. Med. Chem. Lett.* **2008**, *18*, 4068–4071. [CrossRef] [PubMed]

39. Berman, H.M.; Westbrook, J.; Feng, Z.; Gilliland, G.; Bhat, T.N.; Weissig, H.; Shindyalov, I.N.; Bourne, P.E. The Protein Data Bank. *Nucleic Acids Res.* **2000**, *28*, 235–242. [CrossRef] [PubMed]

40. Morris, G.M.; Goodsell, D.S.; Halliday, R.S.; Huey, R.; Hart, W.E.; Belew, R.K.; Olson, A.J. Automated docking using a Lamarckian genetic algorithm and an empirical binding free energy function. *J. Comput. Chem.* **1998**, *19*, 1639–1662. [CrossRef]

41. Molecular Operating Environment (MOE) Chemical Computing Group, Montreal, QC, Canada. 2012. Available online: http://www.chemcomp.com (accessed on 28 February 2013).

Sample Availability: Samples of the compounds are currently not available from the authors.